AMOC fingerprints influence seasonal SST predictability in the North Atlantic

Julianna C. Oliveira[1], Leonard F. Borchert[2,3], Aurélie Duchez[4], Mikhail Dobrynin[3,5], and Johanna Baehr[3]

[1]University of Southampton, Southampton, United Kingdom. *Present address:* Helmholtz-Zentrum Geesthacht, Geesthacht, Germany and International Max Planck Research School on Earth System Modelling, Max Planck Institute for Meteorology, Hamburg, Germany
[2]Sorbonne Universités (SU/CNRS/IRD/MNHN), LOCEAN Laboratory, Institut Pierre Simon Laplace (IPSL), Paris, France
[3]Institute of Oceanography, Center for Earth System Research and Sustainability (CEN), Universität Hamburg, Hamburg, Germany
[4]ESAIP La Salle, Aix en Provence, France and National Oceanography Centre, Southampton, United Kingdom
[5]Deutscher Wetterdienst (DWD), Hamburg, Germany

Correspondence: Julianna C. Oliveira (julianna.carvalho@hzg.de)

Abstract. We investigate the impact of the strength of the Atlantic Meridional Overturning Circulation (AMOC) at 26°N on the prediction of North Atlantic sea surface temperature anomalies (SSTA) a season ahead. We ~~consider the physical mechanism proposed by Duchez et al. (2016a) and~~ test the dependence of SST predictive skill in initialised hindcasts on the phase of AMOC at 26°N, invoking a seesaw - like mechanism driven by AMOC fluctuations. We use initialised simulations with the

5   MPI-ESM-MR seasonal prediction system. First, we use ~~the~~ an assimilation experiment between 1979-2014 to confirm that the AMOC leads a SSTA dipole pattern in the tropical and subtropical North Atlantic, with strongest AMOC fingerprints after 2-4 months. Going beyond previous studies, we find that the AMOC fingerprint has a seasonal dependence, and is sensitive to the length of the observational window used, i.e. stronger over the last decade than for the entire time series back to 1979. We then use a set of ensemble hindcast simulations with 30 members, starting each February, May, August and November between

10   1982 and 2014. We compare the changes in skill between composites based on the AMOC phase a month prior to each start date to simulations without considering the AMOC phase. We find higher SST hindcast skill at 2-4 months lead time for SSTA composites based on the AMOC phase for February, May and November start dates. Our method shows major benefit for May start dates, where mean summer SST hindcast skill over the subtropics ~~increase~~ increases by a factor of 2, reaching up to 80% agreement with ERA-Interim SST.

1   Introduction

15   ~~The variability of SST~~Sea surface temperature (SST) variability at seasonal timescales has a significant impact on the weather and climate (Stockdale et al., 2011; Sutton and Hodson, 2005). ~~Tropical seasonal~~ Seasonal SST anomalies (SSTAs) in the tropics have been linked to the intensity and genesis of tropical cyclones and heatwaves (Coumou and Rahmstorf, 2012; Duchez et al., 2016b; Arora and Dash, 2016), and to fluctuations of marine resources (Stock et al., 2015); all of which have

20   ~~the potential of~~ potentially important socio-economic consequences. Nevertheless, the mechanisms governing ~~seasonal SST~~

predictability of seasonal SST changes are not well understood (Stocker, 2014). Correspondingly, seasonal predictions of SSTAs often show low skill, particularly over the extratropics (e.g. Arribas et al. (2011)).

Air-sea heat fluxes (ASFs) and Ekman-induced oceanic heat transport are important drivers of seasonal variability for SSTs (Bjerknes, 1964; Gulev et al., 2013). The North Atlantic Oscillation (NAO) is recognised as the main mode of climate variability at seasonal to interannual timescales in the North Atlantic (Deser et al., 2010), and a SST anomaly tripole is seen as its major imprint on the ocean surface (Marshall et al., 2001). Part of the North Atlantic seasonal SST variability has also been attributed to the AMOC (e.g. Bryden et al. (2014); Zhang et al. (2019)). The AMOC is estimated to transfer about 1.3 PW (10^{15} W) of heat northwards at 26°N (Johns et al., 2011). This heat transport, however, shows little meridional coherence at seasonal to interannual timescales (Bingham et al., 2007; Hirschi et al., 2007). Through local convergence or divergence of ocean heat transport (OHT, e.g. Cunningham et al. (2013); Borchert et al. (2018)), AMOC fluctuations could therefore influence the seasonal to interannual predictability of SST. The SST response to AMOC results in recurring large-scale patterns, generally known as AMOC fingerprints (Zhang, 2008).

Here, we examine the seesaw mechanism proposed by Duchez et al. (2016a) (henceforth D16), which links variations in strength of the Atlantic Meridional Overturning Circulation (AMOC) at 26°N and North Atlantic SSTs on monthly time scales. We evaluate to what extent the seasonal SST predictive skill in the North Atlantic is sensitive to the phase of AMOC before the prediction is made. D16 analysed the relationship between AMOC observations at 26°N (Smeed et al., 2014) and ERA-Interim SST (Dee et al., 2011) during 2004-2014, finding a strong SST dipole pattern centred at 26°N following AMOC anomalies at 3-5 months lag. D16 proposed a dipolar response of SSTs to AMOC variability, in which a stronger than average AMOC at 26°N advects more heat northward, leading to colder waters in the tropics and warmer waters in the subtropics. Conversely, a weaker AMOC advects less heat northward of 26°N, building up heat south of 26°N, and leading to colder waters to the north and warmer to the south of 26°N. Hence, AMOC variations at 26°N were suggested as a precursor to SSTAs in the tropical and subtropical North Atlantic, implying a potential application on seasonal forecast systems.

Recent studies have found improved hindcast skill in the North Atlantic region after considering known physical mechanisms into their seasonal prediction analysis. Mechanisms were invoked in two possible ways: by identifying and explaining times of low and high skill,

including precursors of high skill, as so-called *windows of opportunity* (Borchert et al., 2018; Mariotti et al., 2020); or by establishing physical mechanisms in the hindcast ensemble by sub-selecting ensemble members that meet certain physical criteria, thus filtering atmospheric noise in the ensemble (Dobrynin et al., 2018; Neddermann et al., 2018). The present study focuses on oceanic processes that are arguably less noisy than atmospheric dynamics (Gulev et al., 2013), which is why it focuses on an analysis of windows of opportunity.

~~Seasonal~~ Analysing an ensemble of yearly initialised hindcasts with MPI-ESM-LR covering 1901-2010, (Borchert et al., 2018, 2019) showed that the AMOC at 50°N influences the SST variability and predictability for several years, with higher skill after years of strong AMOC and vice versa. Borchert et al. (2018) perform a predictive skill analysis of SST conditioned to strong and weak OHT anomalies at 50°N separately, showing a robust influence of the ocean on windows of opportunity for decadal subpolar North Atlantic SST predictions. A similar analysis has not yet been performed on the seasonal time scale. Studies suggest, however, an influence of the ocean on seasonal predictability as well. In particular, seasonal SST potential predictability, i.e. the fraction of long-term variability that may be distinguished from the internally generated natural variability, was shown to improve for better represented ocean initial states in the tropical Pacific boreal winter (Alessandri et al., 2010), and in parts of the Atlantic (Balmaseda et al., 2013). ~~When analysing an ensemble of initialised coupled simulations with MPI-ESM-LR covering 1901-2010, Borchert et al. (2018, 2019) showed that the AMOC at 50°N influences the SST variability and predictability for several years~~ We therefore pursue the establishment and explanation of windows of opportunity for seasonal predictions of North Atlantic SST, invoking the seesaw mechanism proposed by D16.

We apply a similar technique as Borchert et al. (2018) to evaluate the impact of the strength of the AMOC at 26°N on seasonal prediction of SST. ~~We use~~ Using simulations from the MPI-ESM-MR-based seasonal prediction system (Dobrynin et al., 2018) ~~, and~~ and invoking the seesaw mechanism proposed by D16, we examine whether predictions initialised following an anomalously strong AMOC event at 26°N are prone to show higher SST predictive skill ~~over the region~~ north of this section. Likewise, predictions initialised after anomalously weak AMOC events at 26°N could show higher SST skill over the tropical region, to the south of this section, due to a local convergence of ~~ocean heat.~~ oceanic heat. Knowledge about connections between SST prediction skill and preceding AMOC strength could be used by decision makers to narrow down the credibility of actual forecasts of North Atlantic SST (Borchert et al., 2019).

The paper is structured as followed: Section 2 describes the datasets and methods used in this paper. We verify the modelled AMOC against RAPID observations in Sect. 3.1. In Sect.3.2 we assess the influence of AMOC strength on seasonal SSTAs considering two different periods, and evaluate the contribution of seasonality and atmospheric processes. We carry out a predictive skill analysis in Sect.3.3, and assess the impact of considering the AMOC strength at the beginning of the prediction. Section 4 provides the discussion, followed by the summary and conclusions in Sect. 5.

2 Model and methods

2.1 Model description and the prediction system

We use ~~seasonal predictions~~ retrospective seasonal predictions (hindcasts) with the coupled climate model MPI-ESM, in its mixed resolution (MR) setup (Baehr et al., 2015; Dobrynin et al., 2018) in the version as used for the CMIP5 simulations (Giorgetta et al., 2013). The oceanic component is the MPIOM ocean general circulation model, formulated on a tripolar grid with poles over North America, Siberia and Antarctica, ~~and horizontal resolution varying with an average~~ with a nominal horizontal resolution of 0.4 degrees and 40 unevenly spaced vertical ~~layers~~ levels (Marsland et al., 2003; Jungclaus et al., 2013). The atmospheric component ECHAM6 runs at T63 horizontal resolution, i.e. approximate horizontal resolution of 200 km with 95 vertical levels, resolving the troposphere and the stratosphere up to 0.01 hPa (Stevens et al., 2013). Ocean and atmosphere are coupled daily without flux adjustments.

~~The prediction system is full-field initialised, using nudging (Dobrynin et al., 2018)~~Initial conditions of the hindcasts are taken from a fully-coupled assimilation experiment with MPI-ESM-MR. In the assimilation experiment, full temperature and salinity fields in the ocean component were nudged (Dobrynin et al., 2018) towards the ORA-S4 reanalysis (Balmaseda et al., 2013). Temperature, vorticity, divergence, and surface pressure in the atmosphere component were nudged towards ERA-Interim (Dee et al., 2011), and the sea ice component was nudged to NSIDC observations (Comiso, 1995).

We use a 30-member hindcast ensemble initialised every February (FEB), May (MAY), August (AUG) and November (NOV) between 1982 and 2014 from the assimilation experiment (Dobrynin et al., 2018). We end our analysis in 2014, in order to compare to D16 using observations. After each initialisation, the ensemble members run freely for 6 months. The 30-member hindcast ensemble was generated by slightly modified initial conditions, using bred vectors in the ocean component with a vertically varying norm that allows for a full depth perturbation of the ocean (Baehr and Piontek, 2014). In the atmosphere, the diffusion coefficient in the uppermost layer is slightly disturbed to generate the ensemble.

2.2 Data Pre-processing and Statistical Methods

To evaluate the long-term SST dipole pattern dependence on AMOC variability, we use the assimilation experiment covering the period of January 1979 to December 2014. We choose the assimilation experiment over observations because of the short ~~record of~~ observational record of AMOC from the RAPID/MOCHA ~~observations~~ array that is available only from April 2004 (Cunningham et al., 2007)~~,~~. Our method therefore allows to constrain the seasonal cycle more ~~accurately.~~ robustly. Comparing our results back to the short observational record allows for an assessment of how model-based and observational dynamics compare. In the model, the meridional overturning transport is directly calculated using the 3-dimensional velocity field averaged at each latitude, and the AMOC is defined as the vertical maximum of the stream function. We verify the modelled AMOC using observations from the RAPID array at 26°N. The RAPID AMOC is defined as the sum of three components: the Florida Strait transport, the surface Ekman transport (EKM), and the geostrophic upper-mid-ocean transport. A detailed description of the calculation of the individual components is provided in Smeed et al. (2018).

We evaluate the atmospheric contribution to the SST variability using ~~EKM and ASF~~the Ekman transport (EKM) and air-sea heat fluxes. We evaluate both the EKM relationship to SST, as well as the AMOC without its EKM component, i.e. AMOC-EKM (Mielke et al., 2013). EKM is calculated from the zonal wind stress component τ_x integrated over the Atlantic, i.e. $EKM = -\int \frac{\tau_x}{\rho f} dx$, where ρ is the reference density (1025 kg m^{-3}) in MPIOM and f is the Coriolis parameter. For ASF we use the total surface heat fluxes over ~~sea~~the ocean, which include shortwave, longwave, latent and sensible heat fluxes. ASF is parameterized as described in Marsland et al. (2003), with fluxes defined positive downward.

To further analyse the influence of AMOC on SST variations, we calculate the convergence of OHT with respect to two latitude bands encompassing a tropical (10.5° - 22.5°N), and a subtropical (28.5° - 40.5°N) region. These latitude bands are the same used to define Box 1 and Box 2 in Fig. 4.a. Following Jayne and Marotzke (2001), we calculate the OHT as the zonal and vertical integral of the heat flux across an east-west section through the Atlantic Basin, i.e.

$$OHT = \rho_o c_p \int\limits_{x_W}^{x_E} \int\limits_{-H(x,y)}^{0} v(x,y,z)\theta(x,y,z)\,dz\,dx$$

where ρ_o is a reference density, c_p the specific heat capacity of sea water, H is the water depth, x stands for longitude and y for latitude, z is the water column depth, x_E and x_W are the eastern and western limits of the section, v is the meridional velocity, and θ is the potential temperature in degrees Celsius.

We calculate monthly means of AMOC, EKM, SSTA and air-sea heat fluxes. Our main data set consists of model output, in addition to AMOC observations from RAPID and 'observed' SST from the ERA-Interim reanalysis (Dee et al., 2011). This data set is deseasoned by removing the 12-month climatology obtained from the monthly data, and the linear trend is removed as an idealised approach to remove the externally forced signal from the time series and focus on internal variability. We refer to these detrended, deseasoned quantities as anomalies. ~~Time series are smoothed using a 3-month running average to filter out high frequency variability.~~ Seasonal means are defined as December-January-February (DJF) for winter, March-April-May (MAM) for spring, June-July-August (JJA) for summer and September-October-November (SON) for autumn.

To assess the variability of the AMOC fingerprint and to evaluate its role on seasonal SST predictability, we perform lagged correlations from 0 up to 12 months, with the AMOC leading SSTA. Additionally, we compute lagged correlations for ASF, EKM and AMOC-EKM leading SSTA to explore the ~~atmospheric contribution~~relative contributions of atmospheric and oceanic dynamics to SSTA changes. For our hindcast skill analysis, we assess predictive skill of the hindcast simulations against the ERA-Interim data with the point-wise Anomaly Correlation Coefficient (ACC, Collins (2002)). ~~Significance is assessed via a bootstraping method~~We calculate statistical significance of our findings using a Monte-Carlo bootstrapping method. The process consists of 1000 bootstraps with replacement on the time-dimension at the 95% confidence level~~using 1000 samples~~.

	AMOC	EKM	AMOC-EKM
MPI-ESM-MR	18.42 ± 2.55 (2.79)	3.08 ± 1.61 (3.36)	15.34 ± 2.28 (2.55)
RAPID	17.02 ± 2.95 (3.90)	3.56 ± 1.46 (2.26)	13.43 ± 0.96 (2.42)

Table 1. Transports mean values, standard deviations and seasonal ranges (in parentheses) for the model (1979-2014) and observed AMOC (2004-2014). All values in Sv.

3 Results

3.1 ~~Model verification for~~ Verification of the AMOC in the assimilation experiment

~~We verify the modelled AMOC and the components EKM and AMOC-EKM to observations as a first step to our analysis. Statistics for AMOC and EKM, as well as AMOC-EKM are shown in Table.1.~~

150 We evaluate the AMOC seasonal cycle using both anomalies and full values. ~~The anomalies are calculated by removing the annual mean of each year (~~To show the spread of the annual climatology, grey lines in Fig. 1.~~a-f) of~~ a, c, e represent anomalies w.r.t. the mean transport of a given year calculated for the full time series (1979-2014), ~~after which the data were~~ and smoothed with a 3-month running average. The observed AMOC shows minimum transport in March and maximum in August (~~c.f.~~ Fig. 1.a, b). Minimum transport for the modelled AMOC is achieved slightly later, in April-May, while it peaks twice in August

155 and December. The seasonal cycle for both the observed and the modelled AMOC agree with the ones discussed by Mielke et al. (2013) using RAPID data from 2004-2010 (Cunningham et al., 2007) and a high resolution MPI ocean model spanning the same period. For EKM (~~c.f.~~ Fig. 1.c, d), the seasonal cycle for observations and model are slightly out of phase, but both show a clear maximum in summer (July-August) and minimum in spring (March-April). The seasonal range for the modelled EKM is 3.36 Sv, compared to ~~lower~~ 2.26 Sv for the observations. The opposite is found for the AMOC seasonal range, which

160 is smaller for model (2.79 Sv against 3.90 Sv, Table 1 ~~1~~). These differences in range and phase for AMOC and EKM can explain the seasonal cycle of AMOC-EKM, with minimum in July and maximum in November ~~.~~ (Fig. 1.e, f). Time series of observed and modelled AMOC~~and EKM component~~, EKM and consequently AMC-EKM are in reasonable agreement ~~and correlate with~~ with a correlation of 0.67 (~~cf.~~ and 0.66, respectively (Fig. 1.g). There is no relevant effect of the mean state on these findings, which is why we use anomalies from now on.

3.2 Impact of AMOC fingerprints on North Atlantic SST variability

3.2.1 The RAPID decade

Here, we compare ~~AMOC fingerprints between~~ the observed AMOC fingerprints discussed in D16 ~~and model for the~~ with those found in the assimilation experiment for the RAPID period April 2004 to March 2014 (c.f. D16's Fig.3). We calculate lagged correlations up to 12 months, with the AMOC leading (Fig. 2 for maximum -month lag).

170 We find that during the RAPID decade a dipole pattern represents the influence of AMOC on Atlantic SST variability in the ~~model~~ assimilation experiment up to 7 months with positive correlation in the subtropical and ~~tropical~~ negative correlation

in the subtropical regions, similar to D16. ~~This~~ Specifically, this pattern is composed of a large zonal band of anticorrelation located between 5 and 26°N, from the African coast towards the Gulf of Mexico, and a smaller positive correlation lobe between 26 and 40°N (Fig. 2). This dominant SSTA correlation pattern evolves over time.

175   Lags 0 and 2 show maximum positive correlations of the order of 0.6 mostly in the western side of subtropical lobe near the US coast, as opposed to maximum negative correlations of similar magnitude mainly at the eastern side of the tropical North Atlantic, close to northwestern Africa. The magnitude of the correlation (anticorrelation) drops to maximum of 0.4 (minimum of -0.5) with increase in lag. ~~In contrast with smaller lags, patterns for~~ With increasing time lag (5-7 months ~~lag show a displacement of the maximum correlation lobes~~ specifically), the subtropical lobe of positive correlation shows a displacement

180 towards the east ~~and west, respectively, suggesting~~ along the approximate circulation path of the northern boundary of the subtropical gyre. This suggests a role for the subtropical gyre in advecting the ~~AMOC fingerprint~~ northern lobe of the seasonal AMOC fingerprint eastward.

    The correlation pattern for the subpolar region is also pronounced, however the strongest negative correlations of -0.4 are only present up to 2 months lag (~~c.f.~~ Fig. 2.a, b). These negative correlations have been previously associated with the NAO

185 imprint in the Atlantic ~~(Fan and Schneider, 2012)~~(Fan and Schneider, 2012; Oelsmann et al., 2020), and are not explained by D16's physical mechanism which we investigate in this study. D16's physical mechanism attributes an active role of ocean heat advection on the SST variability at the timescale of a few months, due to anomalous convergence or divergence of OHT. Therefore, we restrict our analysis to the AMOC influence on SST over tropical and subtropical North Atlantic, and exclude the subpolar pattern from our analysis.

190 ### 3.2.2   Investigating a 30-year period

We now analyse the impact of AMOC on SSTs over the full 36 ~~years~~year period for which the assimilation experiment is available, to assess the consistency of the previous results (Fig. 2) over a longer period. The SST dipole pattern for the full 36-years and RAPID period (Fig. 3) hold mostly similar ~~spatial and temporal~~ spatio-temporal characteristics. The longer period shows, however, lower correlation values than during the RAPID period, particularly over the subtropics and at long lead times

195 >3 months.

    The subtropical lobe shows a consistent ~~maximum positive correlation of the order of 0.2~~ positive correlation throughout lags 1 to 7 months, ~~and a higher correlation of 0.34 for lag 0.~~ with higher correlation at lag 0 (Fig. 3). At lags >3 months, however, these correlation values become statistically insignificant. The tropical lobe of the dipole shows minimum negative correlations ranging from -0.29 and -0.37, which are comparable with the magnitude observed during the RAPID period for

200 the same region. Hence, the SST dipole shows a dependency on the ~~decade~~ time period that is analysed, which is in agreement with ~~Alexander-Turner et al. (2018). We further analyse this dependency~~ findings presented by Alexander-Turner et al. (2018). Analysing this time-dependency further by computing running lagged-correlations for 10- and 15-year windows for lags 1 and 3 months (~~not shown). We~~ see video supplement), we find that the ~~90s~~1990s tend to show a less clear AMOC-SST correlation pattern in comparison to both the 80s and the RAPID period, particularly for the subtropical lobe of the SST dipole.
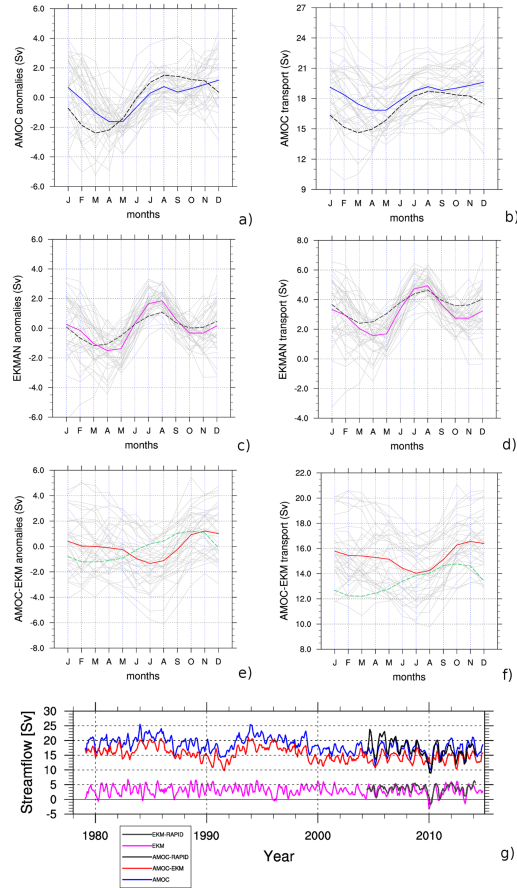
Figure 1. The AMOC in ~~MPI-ESM-MR~~the assimilation experiment. Climatology of the maximum AMOC transport at 26°N in the assimilation experiment, smoothed with a 3-month running mean and the annual cycle removed (spanning 1979-2014), for anomalies (a, c, e), and full values (b, d, f) as labelled. The highlighted full coloured lines represent the mean transport values, whereas each light grey line represents a given year. The dashed lines correspond to the mean value of observed AMOC. g) modelled AMOC at 26°N (blue line), AMOC-EKM (red line) and EKM (magenta line); the observed AMOC (black line) and EKM as the component in the RAPID data (grey line).
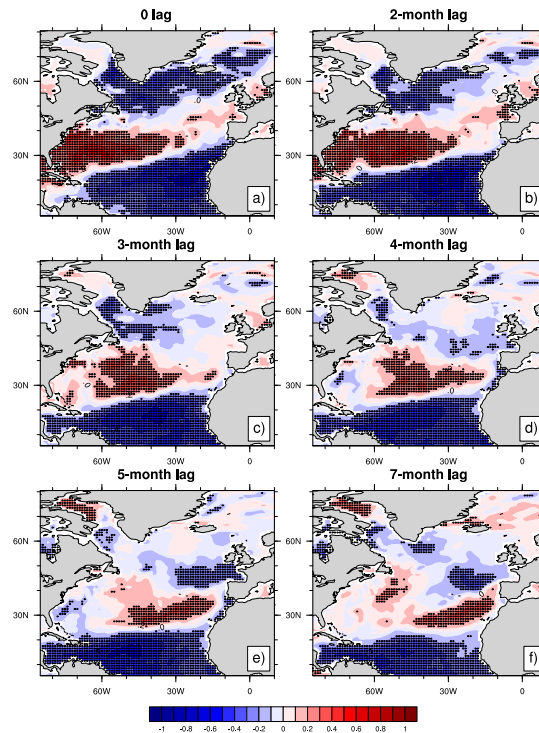
Figure 2. Lagged correlations between AMOC at 26°N and North Atlantic SSTA during the RAPID period (2004-2014), with the AMOC leading (a-f, as labelled) in the assimilation experiment. The stippling represents significant correlations at the 95% confidence level, calculated from 1,000 bootstrap samples.

205   ~~We summarise the main spatial and temporal features of the SST dipole in Fig.4.~~ To further explore the sensitivity of AMOC fingerprints to the length of the observational window used, we show the AMOC-SST relationship averaged over two regions comprising the dipole lobes ~~.~~ (Fig. 4). We define those as tropical lobe: Box 1 (10.5° - 22.5°N, 22° - 55°W), and subtropical lobe: Box 2 (28.5° - 40.5°N, 40° - 70°W, cf. Fig. 4a). We focus on ~~the~~ positive lags, which represent the ~~AMOC~~ AMOC-influenced SST fingerprints.

210   ~~In agreement with Sec.3.2.1,~~Elaborating on findings based on spatial fields (Figs.2,3), we here show spatially aggregated SST variability (Fig. 4). As before, AMOC fingerprints over the RAPID period are stronger than over the full time series. We find high anticorrelations up to 5-month lag over Box 1, ranging from -0.57 at 5-month to maximum magnitude of -0.69 at 2-month lag. In contrast, when the full time series is considered, values drop to the order of -0.4. This results in a significant skill difference between the RAPID and the full period for lags 1-5 months, evaluated by non-overlapping uncertainty envelops for

215   the two correlation estimates (Fig. 4c). Similarly, we find high correlation values above 0.6 up to 2-month lag over the RAPID period for Box 2, which drop to 0.24 at 5-month lag. The magnitude of correlations for Box 2 over the full time series reaches
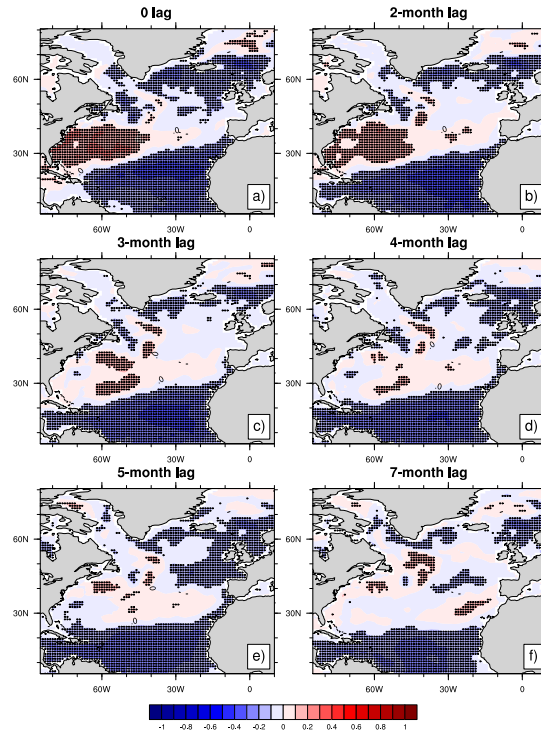
Figure 3. Lagged correlations between AMOC at 26°N and North Atlantic SSTA during 1979-2014, with the AMOC leading (a-f, as labelled) in the assimilation experiment. The stippling represents significant correlations at the 95% confidence level, calculated from 1,000 bootstrap samples.

a maximum of 0.25. ~~Weaker AMOC fingerprints~~ Correlation estimates for box 2 are significantly different between the two periods for lags 0-4 months (Fig. 4c). Weakened AMOC fingerprints with reduced correlation of AMOC to SST, particularly during the 90s (as exemplified in the time series for AMOC and SST; Fig. 4b, d), are likely responsible for the decline of the correlations computed for the full time series.

D16's physical mechanism suggests that via convergence (divergence) of OHT in the subtropics (tropics), a strong AMOC at 26°N drives the subtropical and tropical SST variability at a maximum of 2-5 months lead time. To test the physics behind this hypothesis, we assess the convergence of OHT for the latitudinal bands corresponding to Box 1 and 2 (Fig. 4.e, f, respectively). We define OHT convergence as $\delta OHT = OHT_{SouthernBoundary} - OHT_{NorthernBoundary}$, i.e. heat flow into the latitudinal band minus heat flow out of the band (as in Borchert et al., 2018). This analysis shows significant negative correlation of AMOC with OHT convergence in the latitudes of the tropical lobe (Fig. 4e), showing that AMOC-related outflow of heat represents a significant driver of heat convergence changes in the area. Further, AMOC is weakly positively correlated to OHT convergence in the latitudes of the subtropical lobe of the AMOC fingerprint, indicating a weak but sustained impact of
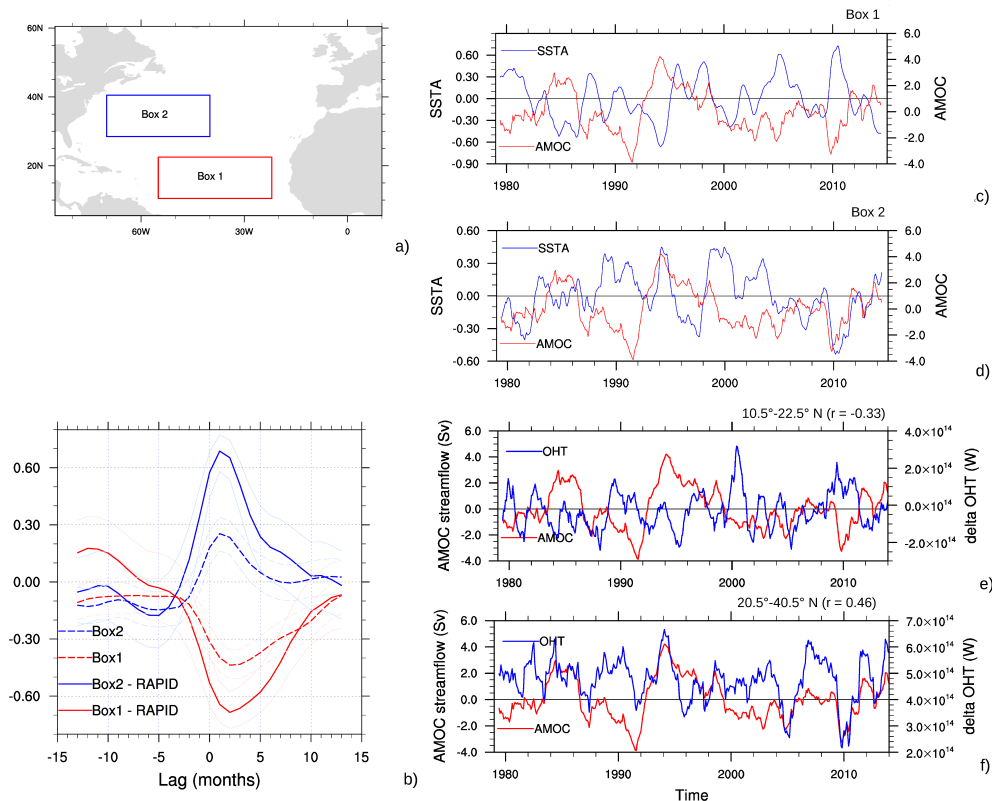
Figure 4. Relationship of AMOC ~~and~~ at 26°N, SSTA and δ OHT over two regions in the North Atlantic in the assimilation experiment: a) regions used for ~~the calculation~~averaging SST; b) lagged correlations between AMOC and SSTA over Box 1 (red lines) and Box 2 (blue lines). Bold lines correspond to the RAPID period~~and~~, dashed lines to 1979-2014, and light colours show the significance at 95%; c) time series for AMOC and SSTA ~~extracted in region~~ averaged for Box 1 and d) for ~~region~~ Box 2, both smoothed with a 12-month running mean; time series for AMOC and δ OHT w.r.t. e) 10.5° - 22.5°N, and f) 28.5° - 40.5°N.

AMOC-related heat transport on oceanic heat convergence there. This could be explained by the relatively small and spatially
230   variable area that is covered by the subtropical lobe of the fingerprint, as the latitude band also covers substantial areas that
are not characterised by the AMOC fingerprint. While a detailed heat budget for the exact boxes studied here would certainly
be interesting, its calculation is complex and beyond the scope of this work. For now, OHT convergence analysis indicates an
influence of AMOC on oceanic heat accumulation south and (less so) north of the AMOC latitude, but also illustrates that other
factors contribute to accumulation of heat in the ocean that overturning does not account for. In this study, however, we will
235   continue to study the AMOC as a predictor of SST, with the accompanying limitations point out above.

3.2.3 The seasonal dependence

~~To further investigate~~ Going beyond previous work (Duchez et al., 2016a; Alexander-Turner et al., 2018) in investigating the variability of the SST dipole pattern, we ~~here~~ analyse the role of SST seasonality. Using the assimilation experiment for the period of 1982-2014, we perform correlations of the AMOC anomalies at a given month with the mean seasonal SSTA 2-4 months ahead (Fig. 5). By doing so, we provide a detailed view of the temporal variability of the SST dipole pattern, ~~making it easier to link~~ enabling an assessment of an attribution of the observed pattern to ~~other~~ non-oceanic drivers that could potentially affect the SST variability, such as ASFs or EKM.

We find a strong fingerprint in spring (MAM), with average (maximum) correlation of the order of 0.4 (0.52) (~~c.f.~~ Fig. 5). During summer (JJA), the fingerprint is less pronounced than in spring, with lower average (maximum) correlation magnitudes of around 0.3 (0.44). In contrast, we find that autumn and winter seasons lack a characteristic dipole pattern ~~,~~ (Fig. 5.c, d), showing instead only a narrow region of negative correlations over the subtropics of the order of -0.2 (-0.1) for winter (autumn). ~~In particular, for autumn SSTs (Fig. 5.c) we find significant positive correlations of the order of 0.6 over the subpolar region, suggesting that atmospheric drivers~~ The absence of a dipole pattern in autumn and winter may suggest the influence of atmospheric drivers that could potentially supersede the AMOC fingerprints during ~~this season.~~ these seasons. Moreover, we find similar characteristics for the AMOC fingerprints using the ensemble mean hindcasts (not shown), which is especially relevant for interpreting the SST predictive skill analysis in section 3.3.
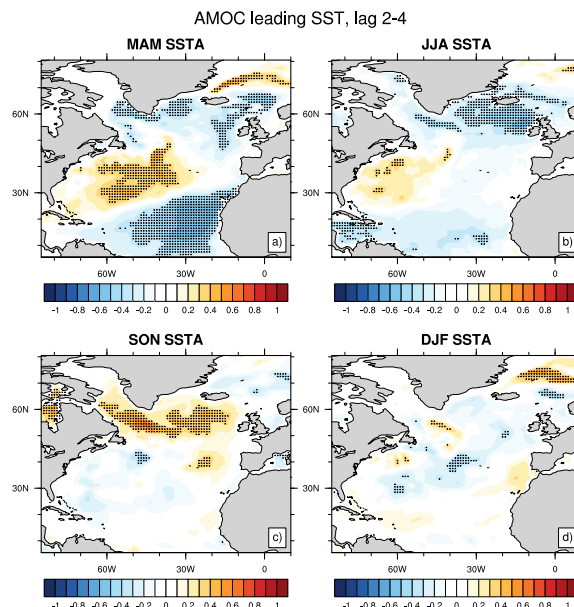
Figure 5. 2-4 month lagged correlations between the SSTA over the North Atlantic and the AMOC at 26°N during 1982-2014, with the AMOC leading (a-d, as labelled) in the assimilation experiment. For example, in a) AMOC in January is correlated to spring SSTAs. The stippling represents significant correlations at the 95% confidence level, calculated from 1,000 bootstrap samples.

3.2.4 The atmospheric contribution

At the seasonal timescale, much of the SST variability in the North Atlantic is the response to atmospheric forcing (Deser et al., 2010). The two main processes responsible for the atmospheric imprint in the large-scale SST variability are anomalous ASFs and EKM-induced oceanic heat transport. The former is known to induce the tripolar SST pattern (Fan and Schneider, 2012), and is mostly forced by the NAO (Cayan, 1992; Marshall et al., 2001). Besides, anomalous EKM may also contribute to the SST variability, especially over regions of strong temperature gradients such as the Gulf Stream (Deser et al., 2010). Fig. 5 shows that AMOC fingerprints have a seasonal dependence. One possible explanation for this seasonality is a stronger atmospheric role on the SST variability in comparison to the AMOC influence, depending on the season. To further explore these interactions, we assess the relative contributions of ASFs and EKM to the SST variability.

We compute correlations between cumulative ASF anomalies and SSTA for 2 and 4 months (where ASF leads) for each seasonal mean SSTA (Fig. 6), thus highlighting regions and seasons where the atmosphere strongly contributes to SST variability. ASFs are defined as positive into the ocean, i.e. positive correlations with SST are interpreted as SST response to atmospheric heat fluxes, and vice versa. Consequently, significant positive correlations between cumulative ASF and SSTA indicate significant atmospheric contribution to SST changes that, should they overlap with AMOC fingerprints identified in Figure 5, indicate a role for the atmosphere in these regions that are potentially unpredictable. As such, this analysis forms an important step towards the assessment of seasonal SST predictions.

We find overall negative correlations between SSTs and ASFs (i.e. ocean forcing to the atmosphere) on the seasonal time scale (Fig. 6), with a few exceptions, e.g. over parts of the Arctic, south of the Azores in summer (Fig. 6c, d) and over the subtropics in autumn (Fig. 6f). We compare these results to Fig. 5, to evaluate whether regions of positive ASF-SST correlations coincide with those of AMOC fingerprints. During spring, summer and winter, regions of significant positive ASF-SST correlations (Fig. 6a-b, c-d, g-h, respectively) do not overlap with the area of strong AMOC fingerprints (cf. Fig. 5a, b, d), suggesting a weak role of ASFs on the AMOC fingerprints during these seasons. In contrast, we note strong positive ASF-SST correlations over the eastern part of the subtropical lobe of the AMOC-SST dipole for autumn (Fig. 6f). This indicates a significant role of ASFs accumulated over 4 months on SST variability for autumn, which partly explains the absence of an AMOC-driven SST dipole over this season, particularly towards the east (cf. Fig. 5c).

In addition to ASFs, Ekman transport is an important contributor to short-term SST variability (Frankignoul, 1985). EKM is the wind-driven component of the overturning
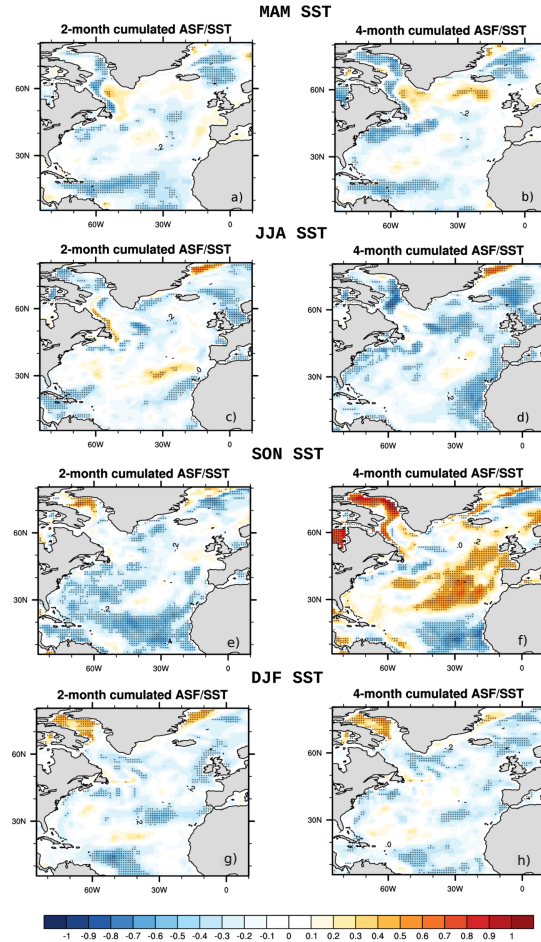
Figure 6. Correlations between the 2 or 4-month ASFs and SSTAs in spring (a and b), summer (c and d), autumn (e and f) and winter (g and h) in the assimilation experiment. As an example, in a) January and February ASF anomalies are correlated to MAM SSTA. The stippling represents significant correlations at the 95% confidence level, calculated from 1,000 bootstrap samples.
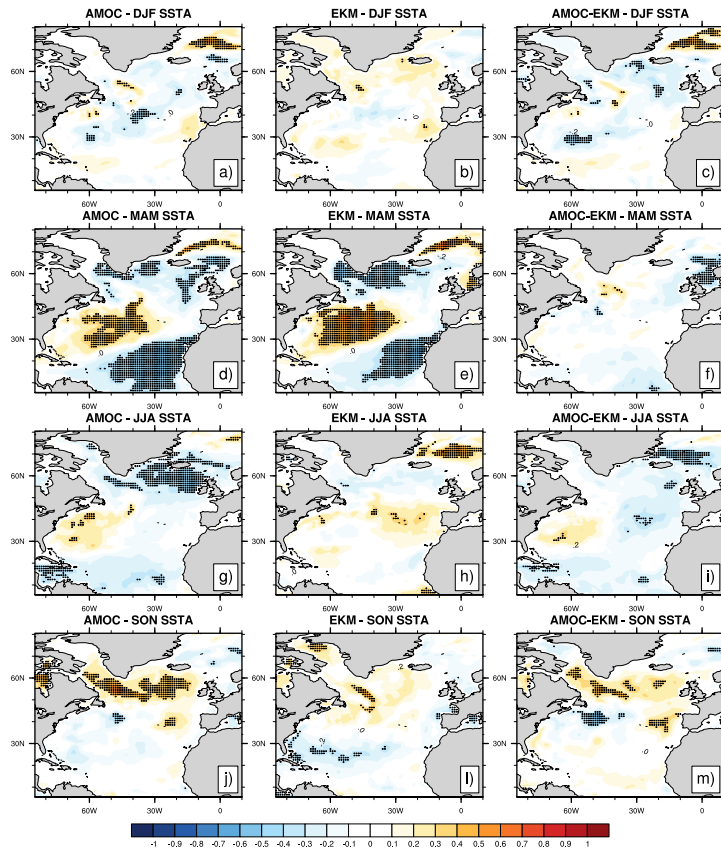
Figure 7. Correlations between SST seasonal means and AMOC (a, d, g, j), EKM (b, e, h, l) and AMOC-EKM (c, f, i, m) at 2-4 month lag (with the transport leading SST) covering the 1979-2014 period in the assimilation experiment. The stippling represents significant correlations at the 95% confidence level, calculated from 1,000 bootstrap samples.

in the ocean, forming the full AMOC signal together with the overturning in the ocean interior, to which usually most of the northward heat transport is attributed (Ferrari and Ferreira, 2011). For spring SSTAs, we find a strong contribution of EKM to the AMOC fingerprint, illustrated by EKM-SST 2-4 month lagged correlations holding a well-define tripole (Fig. 7e), in agreement with D16. For summer SSTAs, however, EKM ~~seems to contribute mainly to~~ weakly contributes to the subtropical

290 lobe of the dipole ~~, given the weak positive correlations in~~ – this contribution is mostly not significant (Fig. 7h. ~~In contrast, the AMOC-SST dipole for both autumn and winter seems to have a distinct main mode of variability less~~). In the other seasons, SST variability seems to be less less influenced by EKM, as shown by the weak correlation pattern for EKM (Figs.7b,l) as well as the high similarity in the SST patterns for AMOC and AMOC-EKM (Figs.7a, c, j, m). ~~The AMOC-EKM contribution for the tropical lobe is significant up to 7 months (not shown), with correlation values of the order of -0.2 similar to the earlier lags~~

295 ~~of 2-4 months.~~

In summary, we present here in further detail the implications of the AMOC fingerprint on North Atlantic SSTs by assessing the atmospheric contribution in terms of cumulative ASFs and EKM on the seasonal SST variability. At time lags where strong AMOC fingerprints occur (2-4 months), we find no significant contribution from the atmosphere in regions of the fingerprints for summer or winter SSTAs. However, autumn SSTAs are strongly affected by cumulative ASFs, which might dampen the development of a clear AMOC fingerprint and therefore could hinder skilful predictions (cf. Fig. 5c). We also find that the EKM component of the AMOC significantly contributes to the fingerprint in spring, with possible implications for seasonal predictions of SST.

3.3 Seasonal hindcast skill

Based on the AMOC fingerprint variability and sensitivity we assessed above, we now test whether considering the AMOC strength at 26°N at the beginning of the prediction may improve the SST predictive skill in the North Atlantic. We particularly focus on the start month dependence of the predictive skill by analysing 30-member hindcast ensembles started every February, May, August and November separately. The hindcasts initialised in FEB, MAY, AUG and NOV yield 2-4 months lead time SST targets MAM, JJA, SON and DJF, respectively. This allows us to build directly on the previously presented results.

All four seasons differ spatially in ACC skill of SSTs for 2-4 months lead time (Fig. 8a, d, g, j). Skill over the subtropics is lower than over the tropics for all start dates. SON and JJA SSTs show the lowest ACCs over the subtropics. Hindcasts show higher ACCs over the tropics than over the subtropics, which is strongest in JJA (Fig. 8g). These results are robust across different lead times, showing similar spatial characteristics, albeit lower skill, for SST ACCs for 3-5 months lead time (not shown).

3.3.1 The role of the AMOC

We now assess the role of the AMOC fingerprints in the SST predictive skill with particular attention to strong and weak phases of the AMOC at 26°N, as dominant AMOC phases imply enhanced memory in the climate system through heat convergence and storage and thus elevated predictability, and vice versa (cf. Fig. 4e, f). To this end, we analyse SST hindcast skill at 2-4 months lead time for phases of strong and weak AMOC at 26°N separately (similar to Borchert et al. (2018). Strong and weak AMOC phases are defined as stronger or weaker than average AMOC a month before the initialisation of the respective hindcast, however our results are not particularly sensitive to the exact choice of

threshold for the definition of strong and weak AMOC phases (not shown). ~~Therefore, we evaluate the impact of AMOC in the~~ ~~SST hindcast skill at 2-4 months time lag, where we find the most pronounced AMOC fingerprints (cf. Sec.3.2). Specifically, we examine local~~ This analysis is performed for all start months separately. We therefore examine changes in the predictive skill ~~over~~ for SST over the tropical and subtropical North Atlantic as modulated by the AMOC through the physical mechanism proposed in D16.

~~D16's physical mechanism suggests that via convergence (divergence) of OHT in the subtropics (tropics), a strong AMOC at 26°N drives the sub- and tropical SST variability at a maximum of 2-5 months lead time. Therefore, as a consequence of the ocean's thermal memory, we expect that hindcasts initialised after strong AMOC phasesmay result in more (less) predictable SSTs in the subtropics (tropics), given weaker contribution from the atmosphere to the SST variability over the areas of strong AMOC fingerprints.~~

~~For strong AMOC phases, we find higher~~ After strong AMOC phases, we find increased hindcast skill for DJF, JJA and MAM SSTAs over the subtropics in comparison to ACCs considering the full period (~~cf.~~ Fig. 8a-b, g-h, d-e~~, respectively), in agreement~~). While this skill is in some cases concentrated in smaller areas, this finding is generally consistent with the physical ~~mechanism. ACCs above 0.6 are found in the Gulf Stream region and along the North Atlantic Current for JJA and DJF SSTAs (cf. Fig.8h, b, respectively).~~ seesaw mechanism from D16. In particular, we find higher skill for JJA SSTAs in a zonal band between 30° - 40°N extending up to 40°W, where mean ACCs increase by a factor of 2 and reach maximum above 0.8 in comparison to ACCs considering the full period (~~cf.~~ Fig. 8g, h). ACCs for MAM SSTA increase over the subtropics particularly in the Sargasso Sea, where ACCs above 0.8 cover most of its western side. While the mechanism does not solely explain the hindcast skill behaviour in the tropics, we find an improvement over the hurricane main development region~~(MDR, ,~~ 10–20°N, 30–60°W, (e.g. Hallam et al. (2019)) with ACCs above 0.8 over large parts (cf. Fig. 8e). For SON SSTAs, prediction skill is not markedly higher after strong AMOC phases than for the full period, which might be related to the strong influence of ASFs during that season (cf. Fig. 6f).

~~We now examine ACC changes in the SST composite based on~~ After weak AMOC phases~~. These~~ , we find weaker changes in hindcast skill ~~, albeit less pronounced than for~~ compared to the full time series that after strong AMOC phases~~,~~ . Still, skill differences we find agree to some extent with D16's physical mechanism for DJF and JJA SSTAs. For example, compared to the full time series (Fig. 8a, g), we find better hindcast skill for DJF and JJA SSTA ~~composites~~ in the tropics, with ACCs above 0.8 mainly occurring over the central ~~MDR (cf.~~ hurricane main development region (Fig. 8c, i~~, respectively). As opposed to these findings, the~~). The physical mechanism fails, however, to explain the ACC changes ~~with respect to SON SSTA composites (cf. Fig. 6~~for MAM and SON SSTA (Fig. 8k, l)~~. This seems to confirm that~~ , where we find generally low skill in both tropics and subtropics.

From the seasonality of the AMOC-SST relationship (cf. Fig. 5), the strongest influence of AMOC on SST skill would be expected during MAM and JJA, with a limited role of AMOC during SON and DJF. Moreover, significant atmospheric contribution to ~~the SST variability (e. g. over the subtropics~~SST variability identified during MAM (from EKM, cf. Fig. 7) and SON (from ASFs, cf. Fig. 6~~e, f) is likely to weaken the AMOC fingerprint for SON SSTAs. Overall, we obtain better hindcast skill for FEB (MAM), MAY (~~) would limit prediction skill as well. The most consistent and clear impact of D16's
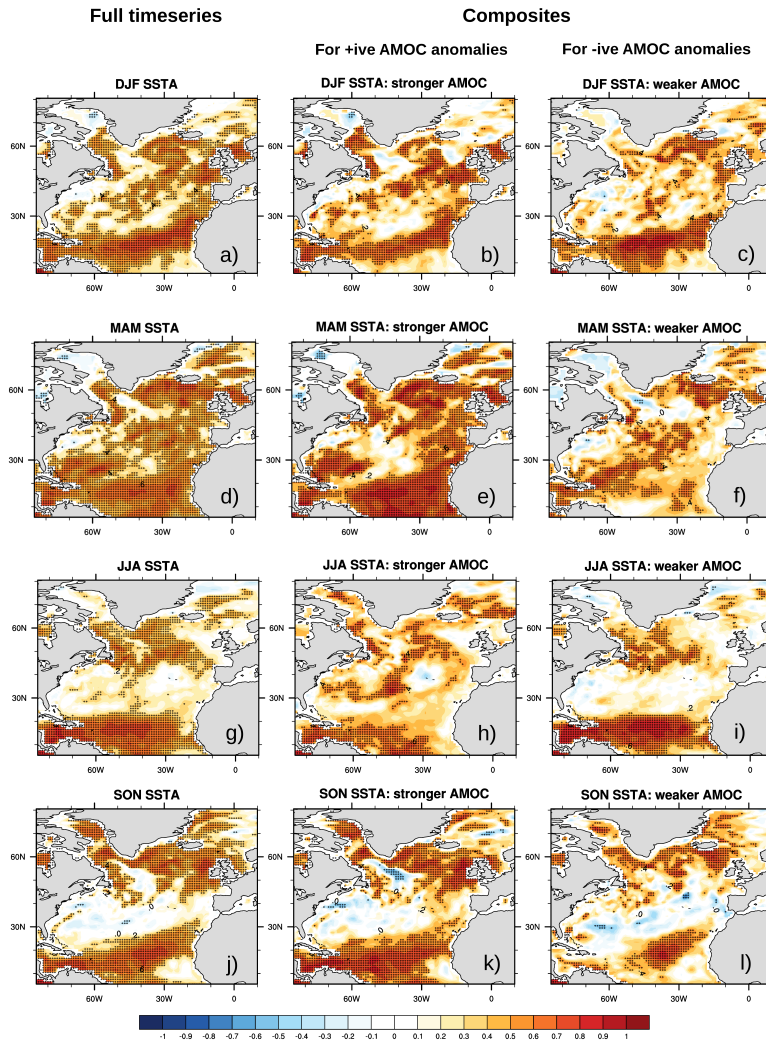
Figure 8. SST ACCs against ERA-Interim at 2-4 months lead time. Leftmost column shows ACCs including the full 33-year time series (1982-2014) for NOV (a), FEB (d), MAY(g) and AUG (j). Next two columns show SST ACCs for composites based on either strong (middle column b, e, h, k) or weak AMOC phases (rightmost column c, f, i, l) 2-4 months before the SST mean, as labelled; e.g. DJF SST composites are based on the strength of AMOC at 26°N in October. Each row shows ACCs for a particular season, starting with winter (DJF) at the top. The stippling represents significant correlations at the 95% confidence level, calculated from 1,000 bootstrap samples.

mechanism on SST skill is therefore to be expected during summer (JJA)~~and NOV (DJF SSTAs) start dates over important~~
~~regions of the North Atlantic, i.e. MDR and parts of the subtropics~~. This is in line with our findings presented here, with the
exception of modest (but likely insignificant) skill increases during DJF. An analysis of area average skill following strong and
weak AMOC phases across season (Fig. 9) confirms this, where only during summer a significant skill difference (defined by
non-overlapping confidence intervals) between strong and weak AMOC phases that is in line with the physical mechanism is
found for both boxes.
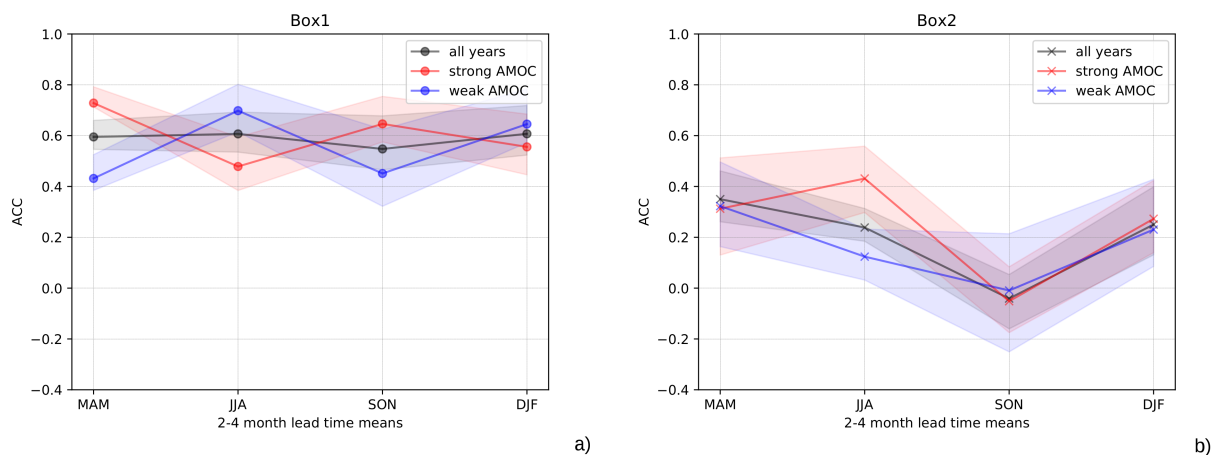
Figure 9. SST ACCs against ERA-Interim at 2-4 months lead time averaged over the regions shown in Fig. 4a. a) Box 1 (10.5° - 22.5°N, 22° - 55°W), and b) Box 2 (28.5° - 40.5°N, 40° - 70°W. Black lines represent the ACCs considering the full time series (1982-2014), red lines for strong, and blue lines for weak AMOC phases. The shaded areas indicate the interquartile ranges.

4 Discussion

While a number of works show evidence for robust AMOC fingerprints on North Atlantic SSTs at decadal and longer time
scales (e.g. Zhang (2008); Muir and Fedorov (2015); Borchert et al. (2018)), only recently the extent to which AMOC influences
SST at seasonal time scales has been addressed ~~(Duchez et al., 2016a)~~(Duchez et al., 2016a; Alexander-Turner et al., 2018). In
this study we explore the influence of AMOC strength at 26°N on North Atlantic SST seasonal variability and predictability
in the MPI-ESM-MR model. We specifically test whether our model AMOC fingerprints agree with the physical mechanism
proposed in D16, and could therefore be considered in ~~our predictions~~ prediction analysis to condition seasonal SST hindcast
skill over North Atlantic tropics and subtropics on the AMOC phase at the start of the prediction. Our findings suggest that
the strength of AMOC is a potential regional source of SST predictability, mainly during summer (JJA), by controlling the
variability of heat advection north or south of 26°N. In other seasons, the impact of AMOC on seasonal SST predictions is

380 limited, for example by strong Ekman transport influence during spring (MAM) and dominant heat fluxes from the atmosphere during fall (SON).

In line with D16, we find pronounced AMOC fingerprints at 2-5 months lag when considering the RAPID period (2004 - 2014). Going beyond this study, however, we find that AMOC fingerprints are sensitive to the length of the observational window used (as also noted by Alexander-Turner et al., 2018). Although our findings are in good agreement with D16

385 when we restrict the analysis to the most recent decade (cf. Fig. 2), we find less pronounced AMOC fingerprints with respect to the full time series back to 1979, at a maximum of 2-4 months lag. A possible reason for these differences could be ~~the decadal AMOC variability , i.e. AMV~~ multidecadal changes in AMOC variability and their imprint on SST (e.g. ~~Ba et al. (2014); Knight et al. (2005)~~Ba et al. (2014); Knight et al. (2005); Borchert et al. (2018)). The RAPID period corresponds to a ~~positive AMV phase (Zhang, 2007), i.e. warmer SSTs~~ period of warm SST over the North Atlantic (Zhang, 2007, we find this in both m

390 , due to changes in the AMOC dynamics at the multidecadal time scale, resulting in stronger OHT that could potentially enhance the AMOC influence at the seasonal timescale.

Alexander-Turner et al. (2018) found a similar time dependence using a 120-year long preindustrial control simulation with HadGEM3-GC2. They tested the robustness of the AMOC fingerprints on the SST through time, finding a good agreement with D16 at the 5-month lag, when taking the mean of 11-year segments of the full time series. However, when considering the full

395 120-year time series, this agreement was overall lower than when analysing the 11-year segments. Likewise, we find weaker AMOC fingerprints when analysing 30-year segments selected from the MPI-ESM-MR historical simulation (not shown).
~~In addition to the sensitivity of the observational window length, a~~ In tandem with the work from Alexander-Turner et al. (2018) , our work therefore illustrates the importance of placing analyses on observed AMOC influence of SST in the broader temporal context using model simulations.

400 A key aspect that distinguishes our analysis from previous studies is that we find a significant seasonal dependence on the AMOC fingerprints. This dependence is coherent in both initialised and free-running model (not shown), with the strongest AMOC fingerprints occurring during spring and early summer. In line with Alexander-Turner et al. (2018), we argue that a main driver for this seasonal dependence is the contribution of stochastic atmospheric variability, and in a lesser extent the Ekman transport. This has a direct implication on the consideration of the physical mechanism in our seasonal prediction

405 system, which is thus dependent on the initialisation month.

The impact of this seasonal dependence can be illustrated as the distinguished effects of the physical mechanism on the hindcast skill for each start month (cf. Fig. 8). Over parts of the subtropics, we achieve high SST hindcast skill for NOV (DJF SSTAs), FEB (MAM), and particularly for MAY (JJA SSTAs), for strong AMOC phases. Our results suggest that summer (JJA) stands out as promising target season for the subtropics, given the relatively weak influence of EKM (strong in MAM)

410 and ASFs (strong in SON), which may decrease the influence of the seesaw mechanism on SSTAs for those seasons. Such windows of opportunity for skilful summer SST predictions (Mariotti et al., 2020) in turn may benefit winter NAO predictions, with consequent influences on the storm track activity starting from October (e.g. Cassou et al. (2004)), as well as on the development of Blocking regimes (e.g. Guemas et al. (2010)), and extreme events (e.g. Arora and Dash (2016)). ~~Moreover, after~~

After weak AMOC phases, we find better hindcast skill for DJF, MAM and JJA SSTAs over the tropics, in particular over the central hurricane main development region. These improved SST predictions over the hurricane main development region could be extremely beneficial for assessing seasonal hurricane formation probabilities (Saunders and Lea, 2008).

Our analysis on AMOC SST variability suggests, however, that enhanced predictability during DJF and MAM is unlikely to originate from AMOC fluctuations, making room for different mechanisms to be explored and discussed in the future. For another example, we highlight that for MAM hindcasts, SSTA skill increases over most of the North Atlantic for strong AMOC SST composites. While these results cannot be explained by D16's mechanism, they suggest that a strong AMOC prior to the start of the prediction in February could potentially overwrite the higher frequency variability of the SST dominated by the atmosphere (e.g. Yeager et al. (2012), Robson et al. (2012) and Borchert et al. (2018)). This supports the evidence of a strong influence of stochastic atmospheric variability for this region at 2-4 months lag (cf. Fig. 6.e-f) and calls for other physical mechanisms, that if incorporated in the prediction could result in a more prominent effect on the hindcast skill. Recently, a similar approach invoked a chain of physical processes in the prediction and achieved improved skill for European summer climate predictions (Neddermann et al., 2018).

As a first step to investigate whether the predictive skill is conditional to the phase of individual AMOC components, we assess the role of the non-Ekman ocean heat transport in driving the seasonal variability of SST. We thus create SST composites based on the AMOC-EKM strength at 26°N for MAY and NOV hindcasts (not shown). Over the subtropics, the Ekman transport is largely responsible for anomalies in the SST, due to its coupling with both strong winds and pronounced temperature gradients (Frankignoul, 1985). Roberts et al. (2017) carried out a detailed observation-based heat budget analysis for short-term variations of the ocean heat content, supporting the idea of potential predictability of SSTs in the mid-latitudes from an active ocean dynamics. Moreover, Ossó et al. (2018) use the ERA-Interim reanalysis and suggest the Ekman advection associated with weaker westerly winds in late winter and early spring to be a major driver of spring SSTA east of Newfoundland. We find a relatively weak improvement on the SST skill over the subtropics for AMOC-EKM SSTA composites, suggesting an important role for the Ekman transport on the predictability of summer and winter SSTs.

Additionally, several studies have shown that one of the most robust remote impacts of ENSO is the teleconnection to tropical North Atlantic SSTs in boreal spring (e.g. García-Serrano et al. (2017)). The incorporation of another physical link into the prediction, such as ENSO, could show additional refined information on the North Atlantic SST prediction skill. Our findings therefore also illustrate that predicting North Atlantic climate on the seasonal time scale is a complex endeavour with plenty of possible drivers of skill that a simplified analysis using just AMOC as skill precursor cannot fully explain.

450   Our analyses support further investigation of the AMOC strength and its associated heat transport as complementary information for the seasonal prediction of SSTAs. Both high-resolution coupled models and the two ongoing AMOC monitoring programs RAPID-MOCHA (Cunningham et al., 2007) and OSNAP (Lozier et al., 2017, 2019) are essential for a thorough understanding of the mechanisms analysed here. In fact, the seasonal relationship between AMOC and SSTA could contribute to the knowledge of the potential applications of a real-time data delivery system, when finally implemented in the RAPID

455   array (Rayner et al., 2016).

5   Conclusions

We assess the impact of AMOC fingerprints on North Atlantic seasonal SST variability and predictability across seasons and time. We consider the physical mechanism proposed by D16 in the hindcast skill analysis of a 30-member ~~ensemble hindcast set~~ of ensemble hindcasts with the MPI-ESM-MR initialised every February, May, August and November, and evaluate the

460   effect of this mechanism by exploring the changes in SST hindcast skill for tropical and subtropical North Atlantic SST, when compared to the hindcast analysis without considering this mechanism. Our findings ~~using MPI-ESM-MR~~ suggest that:

Variability

1. For the period of 1979 - 2014, the AMOC strength at 26°N leads a SSTA dipole pattern in the tropical and subtropical North Atlantic with maximum correlations at 2-4 months, in line with the findings of D16 using AMOC observations

465   from RAPID.

2. ~~In extension to D16, this~~ This AMOC fingerprint has a seasonal dependence, and is sensitive to the length of the time window used. This sensitivity affects both the intensity and structure of the fingerprints, which are stronger in spring and summer than during autumn and winter, and over the last decade ~~,~~ than for the entire time series back to 1979.

3. The AMOC ~~fingerprints~~ fingerprint's seasonality can be attributed to i) the influence of stochastic atmospheric variability

470   on SST via ~~cumulative ASFs~~ atmospheric heat fluxes, which is most pronounced for autumn SST variability over the subtropics~~and seems to weaken~~, weakening the effects of AMOC ~~fingerprints~~ fingerprint; ii) Ekman transport, which explains ~~part of the~~ SST variability over the subtropical lobe of the AMOC fingerprint ~~; except during spring, when the AMOC fingerprint is instead mainly determined by the Ekman component.~~ during spring.

Predictability

475   4. ~~For the period of 1982 - 2014, considering~~ Considering D16's physical mechanism in our prediction skill analysis for the period of 1982 - 2014 results in improved SST hindcast skill for 2-4 months lead time over parts of the subtropical and tropical North Atlantic, ~~for FEB, MAY and NOV start dates~~ mainly during DJF, MAM and JJA.

   (a) For strong AMOC phases at 26°N

i. SST hindcast skill for DJF, MAM and JJA improves over regions of the subtropics as a result of higher influence of the ocean's thermal memory on SST predictability, following a convergence of OHT north of 26°N.

ii. This improvement is ~~more prominent for MAY start dates (JJA SSTA)~~most prominent for JJA SSTA, where mean ACCs increase by a factor of 2 over ~~large~~ parts of the subtropics and reach maximum above 0.8.

iii. ~~The effects on the SST hindcast skill over the tropics for MAY and NOV start dates also confirm D16's physical mechanism by showing local decrease in skill as a result of a divergence of OHT south of 26°N and consequent lower influence of the ocean's thermal memory~~During winter and spring, major skill improvement through AMOC is hindered due to limited influence of AMOC (DJF) and prominent influence of Ekman transport on SST (MAM).

(b) For weak AMOC phases at 26°N

i. Albeit the effect is less pronounced than for strong AMOC phases, SST predictive skill is improved over the tropics for DJF and JJA SSTAs, a result of OHT convergence south of 26°N, in agreement with D16's physical mechanism.

ii. Major ~~improvement takes place~~ skill improvement is found over the central ~~MDR~~hurricane main development region, which could benefit hurricane forecasting systems.

We find the strongest and most consistent SST skill increase from AMOC variability during summer over parts of the subtropical and tropical North Atlantic. This is related to a weak overall AMOC influence in winter, and dominant atmospheric variability during spring (EKM) and autumn (ASFs). Our findings suggest that the strength of AMOC at 26°N has an important influence on seasonal predictability of North Atlantic SSTs. Via D16's physical mechanism, the AMOC strength at 26°N could therefore be used to estimate the expected regional SST skill a season ahead.

Code availability. Model simulations were performed using the high- performance computer at the German Climate Computing Center (DKRZ). All data are stored at the DKRZ in archive and can be made accessible upon request (www.dkrz.de/up). Analysis was performed using NCAR Command Language packages available at https://github.com/NCAR/ncl.

Video supplement. A video supplement related to this paper is available from the repository Technische Informationsbibliothek (TIB) at: https://doi.org/10.5446/50922.

Author contributions. JO wrote the article and performed the analysis. MD ran the simulations. LB, AD, JB and JO conceived the study and contributed to the writing and interpretation of the results.

Competing interests. The authors declare not to have any competing interests.

Acknowledgements. The authors would like to thank Joel Hirschi and Simon Josey for helpful discussions, as well as to the Climate Modelling group at the University Hamburg. This work was funded by the Deutsche Forschungsgemeinschaft (DFG, German Research Foundation) under Germany's Excellence Strategy EXC 2037 'Climate, Climatic Change, and Society' Project Number: 390683824, contribution to the Center for Earth System Research and Sustainability (CEN) of Universität Hamburg (JB). It was further funded by the International Max Planck Research School on Earth System Modelling and by the European Union under Horizon 2020 Project EUCP (Grant Agreement 776613) (LB). JO was supported by the MER consortium under an Erasmus Mundus scholarship. The model simulations were performed using the high-performance computer at the German Climate Computing Center (DKRZ).

510

References

Alessandri, A., Borrelli, A., Masina, S., Cherchi, A., Gualdi, S., Navarra, A., Di Pietro, P., and Carril, A. F.: The INGV–CMCC seasonal prediction system: improved ocean initial conditions, Monthly Weather Review, 138, 2930–2952, 2010.

Alexander-Turner, R., Ortega, P., and Robson, J.: How Robust Are the Surface Temperature Fingerprints of the Atlantic Overturning Meridional Circulation on Monthly Time Scales?, Geophysical Research Letters, 45, 3559–3567, 2018.

Arora, K. and Dash, P.: Towards dependence of tropical cyclone intensity on sea surface temperature and its response in a warming world, Climate, 4, 30, 2016.

Arribas, A., Glover, M., Maidens, A., Peterson, K., Gordon, M., MacLachlan, C., Graham, R., Fereday, D., Camp, J., Scaife, A., et al.: The GloSea4 ensemble prediction system for seasonal forecasting, Monthly Weather Review, 139, 1891–1910, 2011.

Ba, J., Keenlyside, N. S., Latif, M., Park, W., Ding, H., Lohmann, K., Mignot, J., Menary, M., Otterå, O. H., Wouters, B., et al.: A multi-model comparison of Atlantic multidecadal variability, Climate dynamics, 43, 2333, 2014.

Baehr, J. and Piontek, R.: Ensemble initialization of the oceanic component of a coupled model through bred vectors at seasonal-to-interannual timescales, Geoscientific Model Development, 7, 453–461, 2014.

Baehr, J., Fröhlich, K., Botzet, M., Domeisen, V., Kornblueh, L., Notz, D., Piontek, R., Pohlmann, H., Tietsche, S., Müller, W. A., et al.: The prediction of surface temperature in the new seasonal prediction system based on the MPI-ESM coupled climate model, Climate Dynamics, 44, 2723, 2015.

Balmaseda, M. A., Mogensen, K., and Weaver, A. T.: Evaluation of the ECMWF ocean reanalysis system ORAS4, Quarterly Journal of the Royal Meteorological Society, 139, 1132–1161, 2013.

Bingham, R. J., Hughes, C. W., Roussenov, V., and Williams, R. G.: Meridional coherence of the North Atlantic meridional overturning circulation, Geophysical Research Letters, 34, 2007.

Bjerknes, J.: Atlantic air-sea interaction, Advances in geophysics, 10, 1–82, 1964.

Borchert, L. F., Müller, W. A., and Baehr, J.: Atlantic Ocean Heat Transport Influences Interannual-to-Decadal Surface Temperature Predictability in the North Atlantic Region, Journal of Climate, 31, 6763–6782, 2018.

Borchert, L. F., Düsterhus, A., Brune, S., Müller, W. A., and Baehr, J.: Forecast-oriented assessment of decadal hindcast skill for North Atlantic SST, Geophysical Research Letters, 46, 11 444–11 454, 2019.

Bryden, H., King, B., McCarthy, G., and McDonagh, E.: Impact of a 30% reduction in Atlantic meridional overturning during 2009-2010, Ocean Science, 10, 683–691, 2014.

Cassou, C., Deser, C., Terray, L., Hurrell, J. W., and Drévillon, M.: Summer sea surface temperature conditions in the North Atlantic and their impact upon the atmospheric circulation in early winter, Journal of Climate, 17, 3349–3363, 2004.

Cayan, D. R.: Latent and sensible heat flux anomalies over the northern oceans: Driving the sea surface temperature, Journal of Physical Oceanography, 22, 859–881, 1992.

Collins, M.: Climate predictability on interannual to decadal time scales: the initial value problem, Climate Dynamics, 19, 671–692, 2002.

Comiso, J. C.: SSM/I sea ice concentrations using the bootstrap algorithm, vol. 1380, National Aeronautics and Space Administration, Goddard Space Flight Center, 1995.

Coumou, D. and Rahmstorf, S.: A decade of weather extremes, Nature climate change, 2, 491–496, 2012.

Cunningham, S. A., Kanzow, T., Rayner, D., Baringer, M. O., Johns, W. E., Marotzke, J., Longworth, H. R., Grant, E. M., Hirschi, J. J.-M., Beal, L. M., et al.: Temporal variability of the Atlantic meridional overturning circulation at 26.5 N, science, 317, 935–938, 2007.

Cunningham, S. A., Roberts, C. D., Frajka-Williams, E., Johns, W. E., Hobbs, W., Palmer, M. D., Rayner, D., Smeed, D. A., and McCarthy, G.: Atlantic Meridional Overturning Circulation slowdown cooled the subtropical ocean, Geophysical research letters, 40, 6202–6207, 2013.

555 Dee, D., Uppala, S., Simmons, A., Berrisford, P., Poli, P., Kobayashi, S., Andrae, U., Balmaseda, M., Balsamo, G., Bauer, P., et al.: The ERA-Interim reanalysis: Configuration and performance of the data assimilation system, Quarterly Journal of the royal meteorological society, 137, 553–597, 2011.

Deser, C., Alexander, M. A., Xie, S.-P., and Phillips, A. S.: Sea surface temperature variability: Patterns and mechanisms, Annual review of marine science, 2, 115–143, 2010.

560 Dobrynin, M., Domeisen, D. I., Müller, W. A., Bell, L., Brune, S., Bunzel, F., Düsterhus, A., Fröhlich, K., Pohlmann, H., and Baehr, J.: Improved teleconnection-based dynamical seasonal predictions of boreal winter, Geophysical Research Letters, 45, 3605–3614, 2018.

Domeisen, D. I., Butler, A. H., Fröhlich, K., Bittner, M., Müller, W. A., and Baehr, J.: Seasonal predictability over Europe arising from El Niño and stratospheric variability in the MPI-ESM seasonal prediction system, Journal of Climate, 28, 256–271, 2015.

Duchez, A., Courtois, P., Harris, E., Josey, S. A., Kanzow, T., Marsh, R., Smeed, D., and Hirschi, J. J.: Potential for seasonal prediction of

565 Atlantic sea surface temperatures using the RAPID array at 26 [deg] N, Climate Dynamics, 46, 3351, 2016a.

Duchez, A., Frajka-Williams, E., Josey, S. A., Evans, D. G., Grist, J. P., Marsh, R., McCarthy, G. D., Sinha, B., Berry, D. I., and Hirschi, J. J.: Drivers of exceptionally cold North Atlantic Ocean temperatures and their link to the 2015 European heat wave, Environmental Research Letters, 11, 074 004, 2016b.

Fan, M. and Schneider, E. K.: Observed decadal North Atlantic tripole SST variability. Part I: weather noise forcing and coupled response,

570 Journal of the Atmospheric Sciences, 69, 35–50, 2012.

Ferrari, R. and Ferreira, D.: What processes drive the ocean heat transport?, Ocean Modelling, 38, 171–186, 2011.

Frankignoul, C.: Sea surface temperature anomalies, planetary waves, and air-sea feedback in the middle latitudes, Reviews of geophysics, 23, 357–390, 1985.

García-Serrano, J., Cassou, C., Douville, H., Giannini, A., and Doblas-Reyes, F. J.: Revisiting the ENSO teleconnection to the tropical North

575 Atlantic, Journal of Climate, 30, 6945–6957, 2017.

Giorgetta, M. A., Jungclaus, J., Reick, C. H., Legutke, S., Bader, J., Böttinger, M., Brovkin, V., Crueger, T., Esch, M., Fieg, K., et al.: Climate and carbon cycle changes from 1850 to 2100 in MPI-ESM simulations for the Coupled Model Intercomparison Project phase 5, Journal of Advances in Modeling Earth Systems, 5, 572–597, 2013.

Guemas, V., Salas-Mélia, D., Kageyama, M., Giordani, H., Voldoire, A., and Sanchez-Gomez, E.: Summer interactions between weather

580 regimes and surface ocean in the North-Atlantic region, Climate dynamics, 34, 527–546, 2010.

Gulev, S. K., Latif, M., Keenlyside, N., Park, W., and Koltermann, K. P.: North Atlantic Ocean control on surface heat flux on multidecadal timescales, Nature, 499, 464–467, 2013.

Hallam, S., Marsh, R., Josey, S. A., Hyder, P., Moat, B., and Hirschi, J. J.-M.: Ocean precursors to the extreme Atlantic 2017 hurricane season, Nature communications, 10, 1–10, 2019.

585 Hirschi, J. J., Killworth, P. D., and Blundell, J. R.: Subannual, seasonal, and interannual variability of the North Atlantic meridional overturning circulation, Journal of Physical Oceanography, 37, 1246–1265, 2007.

Jayne, S. R. and Marotzke, J.: The dynamics of ocean heat transport variability, Reviews of Geophysics, 39, 385–411, 2001.

Johns, W. E., Baringer, M. O., Beal, L. M., Cunningham, S., Kanzow, T., Bryden, H. L., Hirschi, J., Marotzke, J., Meinen, C., Shaw, B., et al.: Continuous, array-based estimates of Atlantic Ocean heat transport at 26.5 N, Journal of Climate, 24, 2429–2449, 2011.

590   Jungclaus, J., Fischer, N., Haak, H., Lohmann, K., Marotzke, J., Matei, D., Mikolajewicz, U., Notz, D., and Storch, J.: Characteristics of the ocean simulations in the Max Planck Institute Ocean Model (MPIOM) the ocean component of the MPI-Earth system model, Journal of Advances in Modeling Earth Systems, 5, 422–446, 2013.

Knight, J. R., Allan, R. J., Folland, C. K., Vellinga, M., and Mann, M. E.: A signature of persistent natural thermohaline circulation cycles in observed climate, Geophysical Research Letters, 32, 2005.

595   Lozier, M., Li, F., Bacon, S., Bahr, F., Bower, A., Cunningham, S., De Jong, M., De Steur, L., Deyoung, B., Fischer, J., et al.: A sea change in our view of overturning in the subpolar North Atlantic, Science, 363, 516–521, 2019.

Lozier, S. et al.: Overturning in the Subpolar North Atlantic Program: a new international ocean observing system, Bulletin of the American Meteorological Society, 98, 737–752, 2017.

Mariotti, A., Baggett, C., Barnes, E. A., Becker, E., Butler, A., Collins, D. C., Dirmeyer, P. A., Ferranti, L., Johnson, N. C., Jones, J., et al.:

600   Windows of Opportunity for Skillful Forecasts Subseasonal to Seasonal and Beyond, Bulletin of the American Meteorological Society, 101, E608–E625, 2020.

Marshall, J. et al.: A study of the interaction of the North Atlantic Oscillation with ocean circulation, Journal of Climate, 14, 1399–1421, 2001.

Marsland, S. J., Haak, H., Jungclaus, J. H., Latif, M., and Röske, F.: The Max-Planck-Institute global ocean/sea ice model with orthogonal

605   curvilinear coordinates, Ocean modelling, 5, 91–127, 2003.

Mielke, C., Frajka-Williams, E., and Baehr, J.: Observed and simulated variability of the AMOC at 26 N and 41 N, Geophysical Research Letters, 40, 1159–1164, 2013.

Muir, L. and Fedorov, A.: How the AMOC affects ocean temperatures on decadal to centennial timescales: the North Atlantic versus an interhemispheric seesaw, Climate Dynamics, 45, 151–160, 2015.

610   Neddermann, N.-C., Müller, W. A., Dobrynin, M., Düsterhus, A., and Baehr, J.: Seasonal predictability of European summer climate reassessed, Climate Dynamics, pp. 1–18, 2018.

Oelsmann, J., Borchert, L., Hand, R., Baehr, J., and Jungclaus, J. H.: Linking Ocean Forcing and Atmospheric Interactions to Atlantic Multidecadal Variability in MPI-ESM1. 2, Geophysical Research Letters, 47, e2020GL087 259, 2020.

Ossó, A., Sutton, R., Shaffrey, L., and Dong, B.: Observational evidence of European summer weather patterns predictable from spring,

615   Proceedings of the National Academy of Sciences, 115, 59–63, 2018.

Rayner, D., Mack, S., Foden, P., Charcos-Llorens, M., and Campbell, J.: Development of the RAPID MK III telemetry system–a report on the NOC tank-testing and shallow and deep-water field trials, 2016.

Roberts, C. D., Palmer, M. D., Allan, R. P., Desbruyeres, D. G., Hyder, P., Liu, C., and Smith, D.: Surface flux and ocean heat transport convergence contributions to seasonal and interannual variations of ocean heat content, Journal of Geophysical Research: Oceans, 122,

620   726–744, 2017.

Robson, J., Sutton, R., and Smith, D.: Initialized decadal predictions of the rapid warming of the North Atlantic Ocean in the mid 1990s, Geophysical Research Letters, 39, 2012.

Saunders, M. A. and Lea, A. S.: Large contribution of sea surface warming to recent increase in Atlantic hurricane activity, Nature, 451, 557, 2008.

625   Smeed, D., Josey, S., Beaulieu, C., Johns, W., Moat, B., Frajka-Williams, E., Rayner, D., Meinen, C., Baringer, M., Bryden, H., et al.: The North Atlantic Ocean is in a state of reduced overturning, Geophysical Research Letters, 45, 1527–1533, 2018.

Smeed, D. A., McCarthy, G. D., Cunningham, S. A., Frajka-Williams, E., Rayner, D., Johns, W. E., Meinen, C. S., Baringer, M. O., Moat, B. I., Duchez, A., et al.: Observed decline of the Atlantic meridional overturning circulation 2004–2012, Ocean Science, 10, 29–38, 2014.

Stevens, B., Giorgetta, M., Esch, M., Mauritsen, T., Crueger, T., Rast, S., Salzmann, M., Schmidt, H., Bader, J., Block, K., et al.: Atmospheric component of the MPI-M Earth System Model: ECHAM6, Journal of Advances in Modeling Earth Systems, 5, 146–172, 2013.

Stock, C. A., Pegion, K., Vecchi, G. A., Alexander, M. A., Tommasi, D., Bond, N. A., Fratantoni, P. S., Gudgel, R. G., Kristiansen, T., O'Brien, T. D., et al.: Seasonal sea surface temperature anomaly prediction for coastal ecosystems, Progress in Oceanography, 137, 219–236, 2015.

Stockdale, T. N., Anderson, D. L., Balmaseda, M. A., Doblas-Reyes, F., Ferranti, L., Mogensen, K., Palmer, T. N., Molteni, F., and Vitart, F.: ECMWF seasonal forecast system 3 and its prediction of sea surface temperature, Climate dynamics, 37, 455–471, 2011.

Stocker, T.: Climate change 2013: the physical science basis: Working Group I contribution to the Fifth assessment report of the Intergovernmental Panel on Climate Change, Cambridge University Press, 2014.

Sutton, R. T. and Hodson, D. L.: Atlantic Ocean forcing of North American and European summer climate, science, 309, 115–118, 2005.

Yeager, S., Karspeck, A., Danabasoglu, G., Tribbia, J., and Teng, H.: A decadal prediction case study: Late twentieth-century North Atlantic Ocean heat content, Journal of Climate, 25, 5173–5189, 2012.

Zhang, R.: Anticorrelated multidecadal variations between surface and subsurface tropical North Atlantic, Geophysical Research Letters, 34, 2007.

Zhang, R.: Coherent surface-subsurface fingerprint of the Atlantic meridional overturning circulation, Geophysical Research Letters, 35, 2008.

Zhang, R., Sutton, R., Danabasoglu, G., Kwon, Y.-O., Marsh, R., Yeager, S. G., Amrhein, D. E., and Little, C. M.: A review of the role of the Atlantic meridional overturning circulation in Atlantic multidecadal variability and associated climate impacts, Reviews of Geophysics, 57, 316–375, 2019.